Journal of the European Ceramic Society 22 (2002) 1525–1541

www.elsevier.com/locate/jeurceramsoc

Multiscale aspects of the influence of yttrium on microstructure, sintering and creep of alumina

S. Lartigue-Korinek[a,*], C. Carry[b], L. Priester[a]

[a]*Centre d'Etudes de Chimie Métallurgique (CECM) UPR 2801, 15 rue Georges Urbain, 94407 Vitry Sur Seine, France*
[b]*Laboratoire de Thermodynamique et Physico-Chimie Métallurgique (LTPCM) U.M.R. CNRS 5614-INPG/UJF E.N.S.E.E.G, BP 75, 38042 Saint-Martin d'-Hères, France*

Received 21 May 2001; accepted 26 September 2001

Abstract

Yttrium doping induces modifications of the microstructural features and properties of polycrystalline alumina. This paper presents a review of most results on this topic. Experimental and calculated results on yttrium grain boundary (GB) segregation are first described. They include yttrium distribution as a function of grain size and atomic structural configurations around yttrium in GBs. The role of yttrium on the overall microstructure, GB structure, GB defects and grain growth is discussed. The discussion provides a basis for the understanding of sintering phenomena and creep behaviour. Attention is particularly focussed on the effect of the transition between GB yttrium segregation and the occurrence of GB precipitates on the properties of yttria doped alumina.

Keywords: Al_2O_3; Creep; Electron microscopy; Grain boundaries; Sintering

1. Introduction

Creep and sintering behaviour of fine-grained aluminas have been widely investigated. The different mechanisms which may operate during creep are summarized in a map giving the different domains of stress as a function of the grain size.[1] Doping alumina generally has a pronounced influence on its behaviour. Most elements present a low solubility limit in this oxide and thus are segregated at grain boundaries. Magnesium doping of alumina polycrystals yields a high ductility under creep, seen as a superplastic behaviour, which has been attributed to grain boundary (GB) diffusion coupled with GB sliding (GBS).[1] Yttrium doping is well known to have a positive influence on the corrosion resistance of alumina scales[2] and on the creep resistance of polycrystals.[3,4] On the other hand, yttrium has a deleterious effect on alumina sintering by reducing the densification rate.[5]

These effects are obviously due to microstructural changes induced in alumina polycrystals by the presence of yttrium. Many efforts have been made to thoroughly investigate the microstructures by transmission electron microscopy (TEM)[6–9] and Scanning Transmission Electron Microscopy (STEM).[9,10] Furthermore, attempts have been made to correlate the evolution of the microstructures of the deformed samples under creep with micromechanims compatible with the macroscopic behaviour of the samples.[11–14] Similarly, a thorough analysis of the microstructural changes which occur during sintering may allow to understand the micromechanisms of densification.

However, some of the observed phenomena have not been explained until now. For instance, there are still controversies about the role of GBs in the high temperature deformation of fine-grained aluminas. This can be explained by a lack of experimental data and an insufficient understanding of GB structures and the relationship between intergranular structure and intergranular chemistry. In particular, the following questions must be raised:

- Until now the transition between the Y segregated state in a GB to the precipitated state in the form of garnet is not well investigated.
- The way how yttrium segregation and/or precipitation affects the processes usually involved in creep and in sintering is not known.

* Corresponding author.
E-mail address: sylvie.lartigue@glvt-cnrs.fr (S. Lartigue-Korinek).

0955-2219/02/$ - see front matter
PII: S0955-2219(01)00471-X

- Yttrium, either alone or associated to other doping elements or impurities, may modify the structure and chemistry of GBs. These GBs may influence creep and sintering processes according to their geometry and consequently to their structure and to their ability for segregation.
- Is there a contribution of grain deformation to the overall response to creep?
- What are the reactions that occur between lattice dislocations and GBs during the high temperature deformation?

To answer these previous questions a multiscale approach of the Y effect on alumina creep and sintering behaviour is required. Starting with the analyses of the constitutive laws, investigations of the microstructures at the mesoscopic scale—with a statistical aspect—must then be performed. They have to be accompanied by microscopic observations in order to emphasise the micromechamisms and how they are affected by the doping element. Finally, a better explanation of the Y effects may be probably found in the changes of the atomic bonding within the GBs between aluminium atoms and between aluminium and oxygen atoms and their influence on the transport phenomena.

The purpose of this paper is twofold.

- To draw up a complete picture of yttrium's role in alumina by reviewing all experimental evidence and theoretical prediction mainly obtained in the last decade which allow some progress in the understanding of the yttrium doped alumina behaviours.
- To understand the GB phenomena in ceramics based on the knowledge of the GB structure, the GB segregation and of the accommodation phenomena of GB dislocations previously developed on metals.[15]

2. Microstructure of yttrium doped aluminas

This section presents experimental results and predictions from atomistic calculations on the distribution and environment of yttrium in GBs of alumina. The relationship between GB chemistry and GB structure as well as the main features of the yttrium doped alumina microstructures are analysed.

2.1. Grain boundary yttrium segregation

Segregation of yttrium at alumina GBs has been evidenced by a wide variety of techniques.[16–19] Yttrium is isovalent to aluminium ion and its ionic radius ($r=0.093$ nm) is larger than that of aluminium ($r=0.041$ nm). The upper limit of yttrium solubility in alpha alumina is less than 10ppm.[20,21] This low solubility is due to rather high defect formation energy as deduced from ab-initio calculations.[22] The strain energy is the main driving force for GB segregation[19] and first AES (Auger Electron Spectroscopy) results are consistent with segregation of yttrium at monatomic layer levels.[16] SIMS investigations confirmed that a localised enrichment of the dopant occurs at GBs and suggested that the distribution of solute was relatively uniform.[14]

Early investigations by STEM helped establishing the GB yttrium content as a function of grain size for a given nominal yttrium concentration (Fig. 1).[23] During grain growth, the GB yttrium content increases until GBs are saturated with yttrium and precipitation of yttrium aluminium garnet (YAG) compound occurs. An interesting result is that the transition from GB segregation to precipitation at GBs depends only on the grain size, whatever the thermomechanical history of the material. The grain sizes for which the transition occurs have been determined for different yttrium concentrations (2.3 μm for 225 ppm Y/Al and 0.8 μm for 676 ppm Y/Al). Predictions using a geometrical model based on the mass conservation of yttrium during grain growth are in good agreement with the experimental results for both types of microstructures, either displaying only segregation or with precipitation. Starting from these results a general map of the grain size as a function of the atomic ratio Y/Al can be drawn (Fig. 2).[24] The upper part on the right side (square symbols) of the diagram corresponds to the microstructure with precipitates while the lower part on the left side (round symbols) corresponds to the microstructures with only GB segregation. These two regions are separated by a straight line whose slope is equal to (−1).

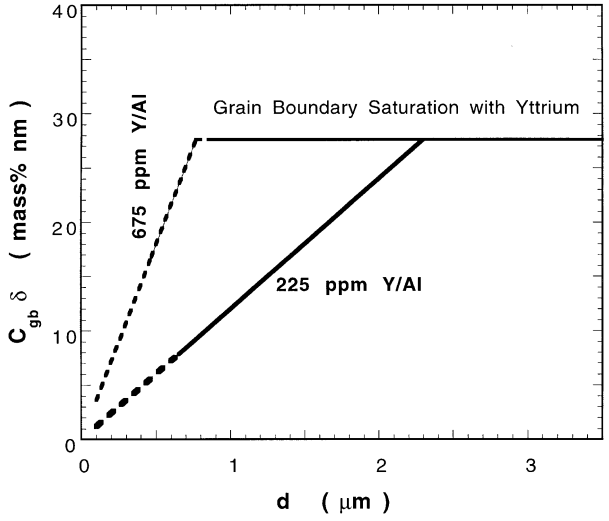

Fig. 1. Schematic diagram of the evolution of yttrium concentration at grain boundaries in fully dense alumina with increasing grain size for two doping levels.[23]

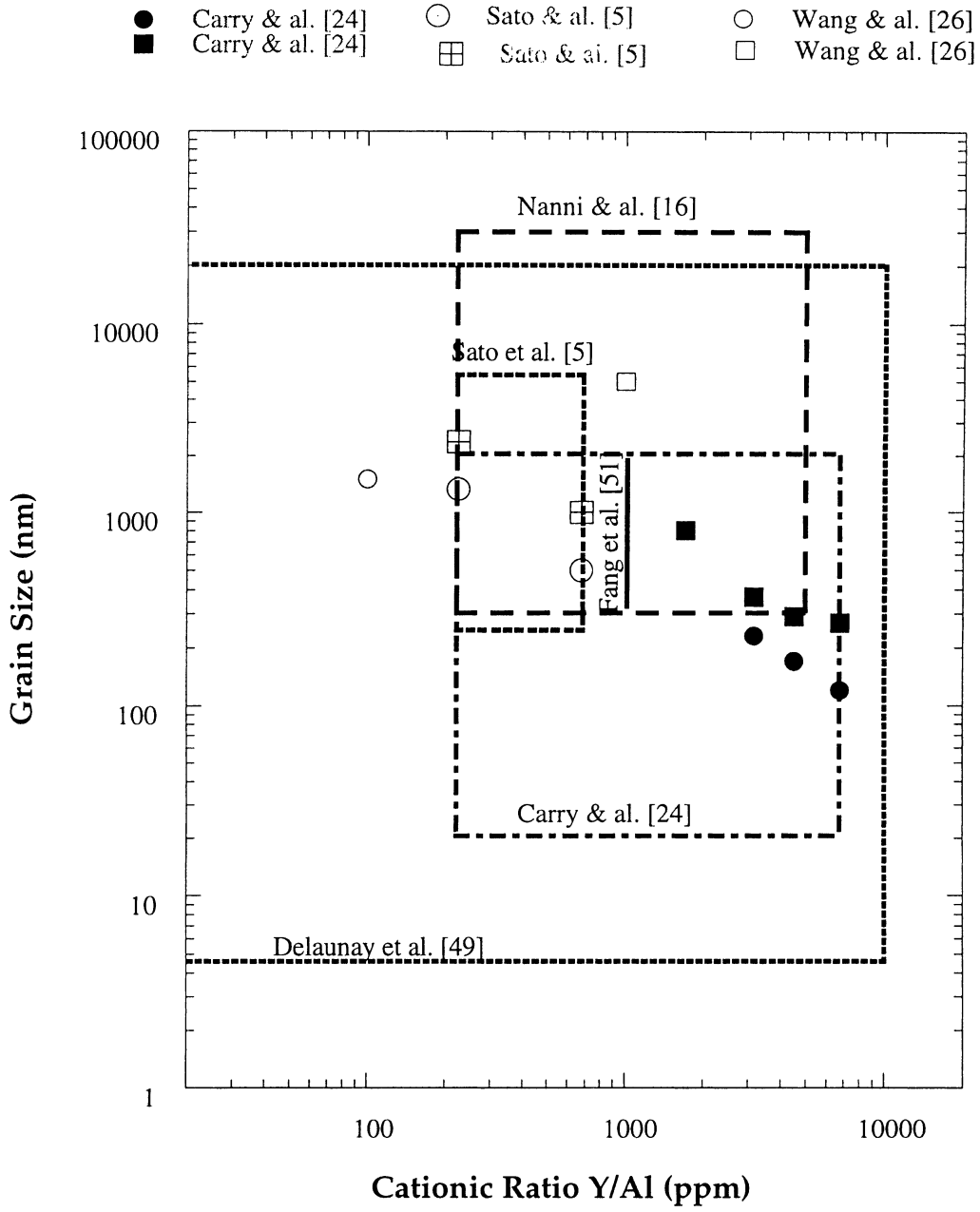

Fig. 2. Diagram showing the grain size versus yttrium doping level on the basis of litterature data concerning grain boundary segregation or precipitation in alumina; square and round symbols correspond, respectively, to microstructures with segregation and precipitation, and to microstructures with only yttrium segregation.[24]

A recent STEM study, using EDXS, on numerous alumina samples doped with increasing amounts of yttrium emphasised the yttrium segregation behaviour:[25] the excess concentration of yttrium at GBs increases with increasing total amount of dopants up to a level (approximately 6 yttrium atoms/nm^2) where precipitation occurs. After the precipitation, the excess concentration is lower (3.5 atoms/nm^2) than the highest measured yttrium excess before precipitation. Thus supersaturation of yttrium occurs on GBs before precipitation. In another work, the highest concentration value at GBs is 5.1 ± 0.2 atoms/nm^2, which corresponds to 1/2 equivalent monolayer. The yttrium concentration drops to a value of 3.2 ± 0.8 atoms/nm^2 after the supersaturation, corresponding to the equilibrium concentration of yttrium in GBs in presence of the YAG phase. Finally chemical composition profiles indicate that yttrium is localised within 2 nm of the GB and the average yttrium content is equal to 4.4 ± 1.5 atoms/nm^2 equivalent to a cation fraction of 9 ± 3 at.%.[10] It is estimated at 6.0 atoms/nm^2 from EXAFS experiments.[26] The supersaturated GBs have been considered to consist of three layers, a disordered core region and a near boundary layer on each side of the GB core. High

resolution images show that the GBs are not disordered beyond one or two atomic planes in materials with low impurity content.[27] A relationship exists between the yttrium supersaturation in GBs and the resulting microstructures that will be discussed further.

In polycrystalline aluminas containing YAG precipitates, EXAFS and STEM investigations attempted to precise the structural and electronic configurations of yttrium ions in the GB. GB bonding states in doped aluminas without precipitation were analysed by EELS. The slight differences which occur in the O–K edge peaks are attributed to a change in the chemical bonding state with the segregation of cations at GBs. Yttrium induces a shift of the peak toward the highest energies in comparison with the peak due to the grain interior. This would reflect a strengthening of GB bonding.[28] EELS analyses suggest that some of the Al ions in GBs containing Yttrium may be tetrahedrally coordinated with oxygen atoms.[29]

Furthermore the distance corresponds nearly to the Y–O bond length in cubic Y_2O_3. Thus the nearest neighbours move outward by 19% of the normal A–O distance. In another work, the number of first oxygen neighbours for yttrium has been found equal to 2.7 at a distance of 0.23 nm and 1.7 at a distance of 0.28 nm.[30] This last shell is attributed to oxygen ions in interstitial positions. The large yttrium ion size induces locally a significant distortion of the oxygen ion lattice that decreases the yttrium coordination number and creates point defects such as vacancies and interstitial oxygen ions.

At this stage *atomistic simulation* can bring insights on the atomic environment in GBs and relationship with segregation. Static lattice calculations of energies and structures of near coincidence GBs emphasised that the coordination number of aluminium atoms in GBs is lower than this number in alumina bulk structure, in agreement with the results of EXAFS experiments.[31] In the intergranular region of a Σ33 GB, there is an increased charge transfer from Al to O, arising mainly from the lower coordination number of the GB atoms, and therefore the reduction in the covalent bond formation.[32]

Lattice Statics, molecular dynamics and Monte Carlo calculations carried out on the basis of empirical potentials indicate that the segregation energy of trivalent dopants is quadratically dependant on the difference in volume between the dopant and the aluminium ions, thus confirming the predominant elastic effect on segregation.[33] This effect is also evidenced from the segregation enthalpy calculations for trivalent dopants in substitution on the largest boundary sites.[34] In the Σ13 boundary, the largest substitutional sites represent 4% of the boundary sites. This value is not in contradiction with the dopant coverage of about 10% experimentally found for general boundaries with probably more opened structures than the Σ13 one. An interesting result is that the segregation energy for a second yttrium is reduced in comparison with this energy for the first yttrium. This indicates that the defects attract each other and form bound agglomerate.[33]

Finally the change in chemical bonding state with doping was estimated by a First principles Molecular Orbital Calculation. The net charges of cations Al^{3+} and O^{2-} are calculated and their product corresponds to the ionic bond strength between Al and O atoms. Yttrium induces an increment in the absolute value of the net charge product showing that the ionicity between the two ions Al^{3+} and O^{2-} increases on substituting an Al^{3+} ion by an Y^{3+} ion.[35] The net charge product seems to be a determinant parameter in high temperature creep of lanthanoid ion-doped alumina.

2.2. Structure and chemistry of grain boundaries

The relationship between GB segregation and GB structure is twofold: on the one hand, the segregated species can modify the crystallographic parameters, and thus the GB structure; on the other hand this structure itself may determine the GB content of segregated species. As a first approximation it has been shown, in experiments with polycrystals and bicrystals on equilibrium segregation in metals, that GBs that present a low segregation are those that display a high mean atomic density at the interface. Segregation is often relatively low at singular boundaries with a large interplanar spacing and a short periodicity, however this trend is not universal. The nature of solvent and solute atoms and the boundary characteristics are important variables that must be considered.[36] The ''GB segregation-structure'' relationship is better understood in metals than in ionic crystals where space charge effects must be taken into account. The situation is even more complex if the studied system contains several solutes. This could be the case for alumina in which residual impurities may not be easily eliminated during powder processing.

In an alumina doped with only yttria, containing a high number of YAG precipitates, yttrium is below the detection limit in a singular boundary Σ3 and in vicinal boundaries very close (0.2°) to the Σ7 orientation relationship. One faceted GB and a general GB with a basal boundary plane in one grain display a low yttrium content.[9]

In aluminas codoped with magnesia and yttria, as well as in aluminas doped with only yttria, containing silicon as the main impurity, yttrium is segregated at nearly all GBs.[37] Yttrium is not detected in one general GB, but its level is high in a low angle GB and in a boundary close to a coincidence orientation relationship. These results prove that there is no reciprocal relationship between three-dimensional coincidence relationship and

intergranular segregation. Indeed the GB plane must be considered as it imposes the GB atomic structure.

Most near coincidence GBs contain dislocation networks. Actually, direct evidence of yttrium segregation on intergranular dislocations has been made.[37] As an example, a general boundary that has shown no continuous segregation contains two isolated dislocations with local yttrium enrichment (Fig. 3). It is assumed that yttrium is attracted by the strain field of extrinsic dislocations that are then stabilised by the segregated species. This result supports the strengthening mechanisms that account for the role of yttrium on creep deformation of alumina, as it will be discussed later on.

Finally a relationship between the GB plane orientation and the nature and the content of segregated species has been evidenced in an alumina with an anisotropic large grain sized microstructure.[37] The large grains correspond to cross-sections of discs whose faces are parallel to the basal plane of alumina, and edges are parallel to other orientations, most often the rhombohedral plane. A preferential segregation of yttrium occurs in GBs whose plane is parallel to the $(01\bar{1}2)$ plane in one grain; silicon is highly segregated at GBs parallel to the basal plane in one grain, although yttrium segregation is relatively low, in agreement with the results of previous study.[9] This indicates that the driving force for segregation of this aliovalent solute also includes charge effects. Atomistic calculations of segregation enthalpy of Y^{3+} exist for surface segregation phenomena. They must be considered with caution when GB segregation is concerned. An interesting point is that they predict large reductions in surface energy for $(01\bar{1}2)$ and $(01\bar{1}0)$ surfaces and virtually no change for the (0001) surface. Moreover a minimum in the heat of segregation occurs at half coverage of $(01\bar{1}2)$ plane that suggests the formation of a coherent second phase at this surface.[38]

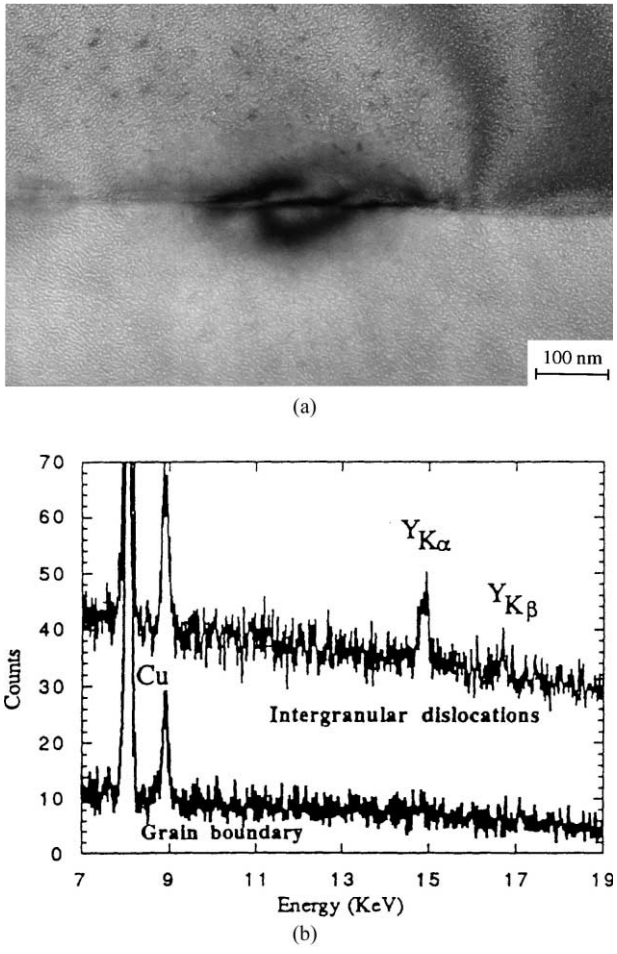

Fig. 3. Detection of yttrium on two GB dislocations.[37] (a) Bright field image of a general GB containing two isolated dislocations; (b) EDXS spectra obtained on two parts of the GB:Y is only detected in the part containing dislocations.

2.3. Microstructural features in yttria doped alumina

2.3.1. Main microstructural features

As expected, overall microstructural features in alumina depend on the total amount of the dopant, and whether yttrium is segregated at GBs or engaged in YAG precipitates, this latter being a function of the grain size and total yttrium content. They are also influenced by residual impurities such as silicon. Generally, lightly doped aluminas without precipitation display a uniform grain size (Fig. 4), whereas a bimodal distribution of grain sizes occurs for highly doped alumina, the precipitates being preferentially localised in the fine grained areas.[9,26] Detailed investigations of the microstructure and microchemistry of polycrystalline alumina doped with varying amounts of yttrium indicate that an explosive jump in the grain size occurs for high yttrium doping level and is linked to transition between supersaturation and precipitation.[25] The microstructure of the samples with segregation is made up of small grains of uniform size (1–2 μm), and the grain size in the samples with precipitates is more than one order of magnitude larger but yet uniform. However, this

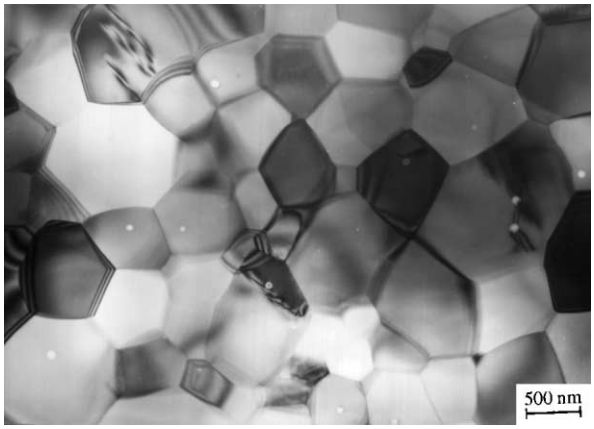

Fig. 4. Microstructure of the fine grained ($d=0.65$ μm) as sintered alumina (225 Y/Al ppm cation, 500 ppm MgO).

"bimodal uniformity" is not observed in samples that contained silicon and calcium impurities and exhibited exaggerated growth of plate-like grains, most often observed in alumina without Mg doping. This feature may be linked to the preferential segregation of silicon in the basal type GBs terminating these elongated grains and highlights the determining role of silicon in the development of such anisotropic grain shape.[37] Finally, the heat treatment atmosphere can strongly modify the final microstructure. For same yttrium content, the microstructure is bimodal with precipitates in air although it is fine-grained equiaxed under low oxygen pressure conditions that induce a larger solubility of yttrium in alumina bulk.[39]

2.3.2. GB crystallographic parameters and features

GB crystallographic parameters were analysed in undoped alumina, alumina codoped with magnesium and yttrium and alumina only doped with yttrium. Transmission electron microscopy studies have shown that large grained undoped aluminas display a low proportion of near coincidence GBs, close to a theoretical distribution of GBs determined for a random distribution of grain orientations.[40,41] This is also the case for aluminas doped with only yttria that had a similar microstructure like undoped aluminas.[37] In microstructures displaying an exaggerated growth of lathlike grains, about half of the GBs are parallel to the basal plane in one grain.

These results are confirmed by statistical determination of GB misorientations by using electron backscattered Kikuchi diffraction.[42] In this last study, GBs close to a near coincidence description according to the Brandon criterion were considered as "special".[43] The crystallographic symmetry in alumina was assumed as hexagonal. In the studies by Lartigue et al., the near coincidence GBs are defined by considering the correct rhombohedral symmetry of alumina[44] and also include boundaries that present a matching of dense planes across the interface. Furthermore, the classification of GBs as near coincidence GBs is made on the basis of the presence of periodic networks of intrinsic dislocations and not only on the basis of a geometrical criterion. This last point will have importance when analysing the micromechanisms of deformation (Section 4.3). However, the results are roughly similar in the two studies.[40,42] On the contrary, the results from aluminas codoped with magnesium are somewhat different. Fine-grained aluminas containing only magnesium display a relatively high number of near coincidence GBs. In aluminas codoped with magnesium and yttrium, this is the case for only the smallest grain size sample (0.65 μm). All the other samples with larger grain sizes contain few near coincidence GBs.

These results indicate that yttrium has a complex influence on microstructural features and thus on related properties of sintered alumina polycrystals as will be described in the next sections.

3. Sintering

Since the successful demonstration by Coble that fully dense transparent alumina can be produced by sintering in the presence of small amounts of magnesia,[45] the influence of solutes on alumina sintering behaviour has been the subject of extensive investigations. During sintering, two main mechanisms can contribute to a decrease in the grain surface area or the grain boundary area: the grain or particle coarsening which occurs at the beginning of the sintering of a fine grained compact and the grain growth in the final step when the porosity does not limit the grain boundary migration.

Chronologically, yttrium is firstly described as a possible beneficent doping element for alumina in a 1968 US patent.[46] It was claimed that "the preferred additive is yttria in combination with magnesia, 0.05% Y_2O_3 plus 0.05% MgO being outstanding". It was further stated that "with this combination alumina bodies can be attained having a density of 3.99, alumina crystal size of about 2–3 μm and with commensurately excellent mechanical strength and other properties". The grain size range for this yttrium doping level corresponds exactly to the grain boundary saturation with yttrium as it was firstly experimentally evidenced 25 years later.[23] In mid 1970s, US patents by Japanese teams proposed the range of 0.05–0.5% by weight of Y_2O_3 as an optimum for properties.[47,48] Finally, minor additions of Y_2O_3 produced some apparent beneficial effect on the shrinkage of alumina compacts attributed to an increase in the diffusion rate.[49]

Later, it was found that addition of yttrium reduces the sintering rate, effect which is attributed to the GB segregation of this element.[16,50,51] The claim of a decrease in densification rate due to Y-doping compares favourably with the observed decrease in creep rates as it will be discussed in the next section.

In an attempt to understand these contradictory results, careful analyses of the sintering behaviour coupled to microstructural investigations have been performed on yttrium doped alumina (225 and 775 ppm Y/Al) codoped with magnesia (500 ppm MgO).[52]

Constant heating rate dilatometric experiments revealed that the main densification rate peak is shifted toward higher temperature for yttrium-doped compacts. Apparent activation energies of the intermediate stage of sintering increase with the yttrium content of the powder. In addition, yttria doped aluminas systematically exhibit an anomalous densification rate peak at temperatures which decrease with the increase of the global yttrium content (Fig. 5). This anomalous peak is also observed in isothermal sintering conditions.[53]

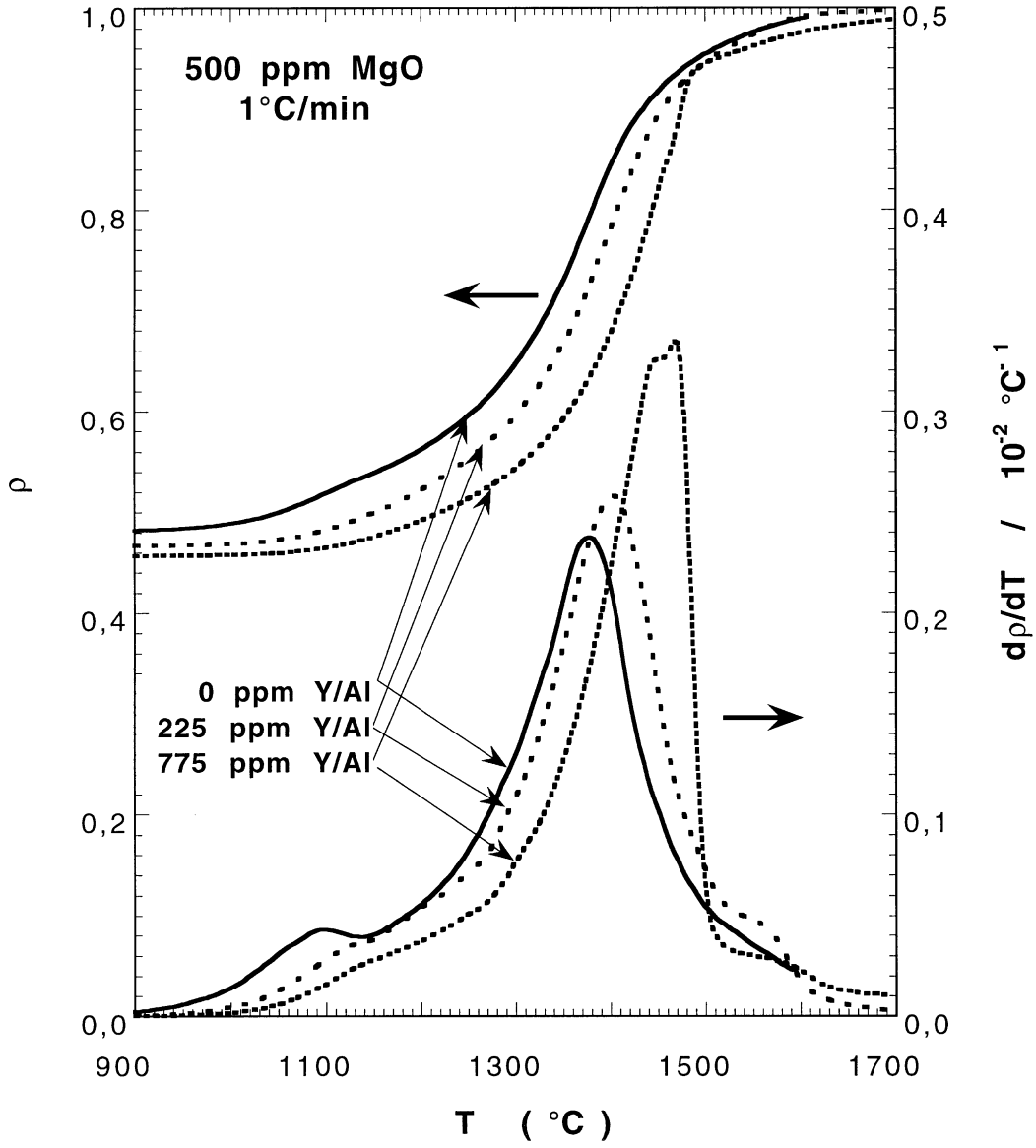

Fig. 5. Sintering behaviour of yttrium doped alumina: an anomalous secondary densification rate peak is observed.[5]

Actually these anomalous peaks correspond to a microstructural transition from GB yttrium segregation to YAG precipitation. Within the anomalous peak, yttrium GB segregation near the saturation level increases the densification.[5] Similar effect of yttrium (from 670 up to 6700 ppm Y/Al) has been found recently for sintering experiments starting from gamma alumina.[24] The anomalous densification rate peak occurs at a lower temperature for higher yttrium content. Also the grain size corresponding to this peak decreases linearly with increasing yttrium doping level.

Although the hot pressing technique was widely used to prepare dense Y-doped samples, until now no study has focussed on the microstructural evolution of these aluminas during sintering. For example, highly doped aluminas present a bimodal microstructure and a heterogeneous distribution of the YAG phase.[9,26] Such characteristics could result from the transient increase in the diffusional mechanisms rather than from an uncontrolled doping process. This will be discussed in the last section. The influence of yttrium on the overall microstructure and sintering will be correlated to the complex creep behaviour of Y-doped aluminas presented in the next section.

4. Role of yttrium in creep of alumina polycrystals

Since fifteen years[54] it is experimentally well established that yttrium decreases the creep strain rate of alumina. Besides, the improvement of fracture toughness at room temperature is significant in yttria doped alumina.[28,55] This behaviour is attributed to the segregation of yttrium at GBs. In case of high temperature

creep, small grain sizes are achieved and the general behaviour is a structural superplasticity. Before analysing the role of yttrium on creep, it is useful to recall the physical models that may account for the observed behaviour at both mesoscopic and microscopic levels.

4.1. Creep processes of fine-grained alumina

As in most superplastic materials, the predominant creep process of fine-grained alumina is a GB diffusion accommodated GB sliding.[1,56] The micromechanisms of deformation are consistent with a "GB dislocation/creep model".[57,58] GB sliding occurs by the glide/climb of GB dislocations in the GB plane. These dislocations result from the interaction of lattice dislocations with GBs or may be created directly in the GBs. The local stress concentrations may be relaxed by incorporation of the extrinsic dislocations in the intrinsic dislocation network or by emission of dislocations into the crystal.[59] In the latter case, the emitted dislocations may or not be absorbed by other GBs. This may induce or impede further GB sliding. Our previous works on Mg-doped aluminas have emphasized the activity of dislocations during creep.[7] The role of GBs as sources and sinks for vacancies and dislocations is a function of the GB structure and chemistry. Diffusion controlled accommodation of extrinsic dislocations may be limited in near coincidence GBs. Dislocations may then be arranged in pseudoperiodic networks, characteristic of a "non equilibrium" configuration. Such dislocation arrays are effectively observed in numerous near coincidence GBs of the deformed samples, although they are scarcely observed in as pressed and annealed samples.[7,8] It is highly likely that near coincidence GBs keep the trade of phenomena that have occurred in all GBs but are not evidenced by TEM in general GBs owing to their rapid recovery.

These intergranular processes have been taken into account in a phenomenological approach that predicts all the observed macroscopic laws as well as the classical features of superplasticity. This physical model postulates for the appearance of fluid-like regions in the GBs subjected to the flux of lattice dislocations. These fluid-like portions result from the spreading of the dislocation cores increasing the free volume. Note that an excess concentration in vacancies has been experimentally evidenced in sliding GBs of superplastically deformed alloys.[60] At the corners of the fluid like regions with the crystalline GB regions, emission of lattice dislocations occurs to relieve stress concentration.[61] The rate of GB deformation $\dot{\varepsilon}_b$ has two components with: $\dot{\varepsilon}_b^{-1} = \dot{\varepsilon}_s^{-1} + \dot{\varepsilon}_a^{-1}$. $\dot{\varepsilon}_a$ is the rate of accommodation at triple points, and $\dot{\varepsilon}_s$ is a composition of rates of rest portion and fluid like portion of the GB. The model allows calculating the contributions of different deformation processes viz. GB sliding $\dot{\varepsilon}_b$, intragranular deformation $\dot{\varepsilon}_v$ and diffusional creep $\dot{\varepsilon}_{cr}$: $\dot{\varepsilon} = \dot{\varepsilon}_b + \dot{\varepsilon}_v + \dot{\varepsilon}_{cr}$. During creep, the role of intragranular slip is reduced such as to maintain superplastic state of GBs and to accommodate the GB sliding. The plastic flow is nearly Newtonian and a low density of lattice dislocations is observed.

It is worth noting that this model considers GB behaviour at a mesoscopic scale: it concerns "general" boundaries that are claimed to be disordered at the atomic level to justify the viscous nature of the plastic flow. However in singular and vicinal boundaries, the accommodation processes involve incorporation of discrete products into the intrinsic network, as inferred in the GB dislocation creep approach. Thus, different types of GBs may answer differently to the deformation, a phenomenon better understood with this approach. Near coincidence GBs were found to be hard elements of the microstructure towards fracture and onsets of cavitation in magnesia doped alumina.[7]

4.2. General role of yttrium on the macroscopic and microscopic behaviour

In the phenomenological equation relating the strain rate to the stress: $\dot{\varepsilon} = A\frac{\sigma^n}{d^p}e^{-\frac{Q_{ap}}{RT}}$, the values of the macroscopic parameters obtained for alumina with various dopant contents and microstructures are summarised in Table 1.[3,4,11,63–71] The stress exponent n is comprised between 1 and 2. The grain size exponent p is generally not reported except in one case where it has been reliably determined.[11] In most studies this coefficient is supposed to be equal to 3 to normalise the strain rates[4] although the microstructure may present in some cases bimodal grain size distributions.[26,27,62] The reported values of the apparent creep activation energies Q_{ap} (Table 1) are systematically higher for yttrium-doped alumina (700–800 kJ/mole) than for non-doped or magnesia doped alumina (450–550 kJ/mole) as illustrated in the Fig. 6 from.[70]

The fact that yttrium decreases the strain rate (by a factor from 3 to 6) was first evidenced in 1987[64] at 1450 °C and confirmed later from tensile tests[65] and compressive tests.[11] More recently other groups reported results at 1250 °C[4,69,70] with a decreasing factor much higher (from 150 to 200) for stresses ranging between 50 and 100 MPa. This striking difference in the reduction of strain rates can be related to the difference in apparent activation energies between non-doped and yttrium doped alumina. In Fig. 6, we have calculated the curves for 20 MPa from the 100 MPa curves using a stress exponent of 2 as reported in the corresponding reference.[70] Fig. 7 shows the experimental strain rate versus grain size curves at 1450 °C under 20 MPa[11] and the corresponding calculated curves at 1250 °C using the apparent activation energies characteristic of the various compositions and grain sizes. This figure clearly shows that the decreasing strain rate factor is much higher at low temperatures.

This beneficial effect on creep properties was also observed for other trivalent dopants.[4,35,70] In 1990 a

Table 1
Main macroscopic parameters from various creep experiments of the literature

Reference	Y/Al (Y_2O_3) ppm	Grain size (μm)[a]	T (°C)	σ (MPa)	TCF	n	Q (kJ/mol)	p	$\dot{\varepsilon}_0/\dot{\varepsilon}$
[63] 1983 (+500 ppm MgO)	225	* 0.6	1500	25–30	C	1.1–1.8			
	(500)								
[64] 1987 (+500 ppm MgO)	225	0.86**–1.93**	1450	25–50	C	1–2			2.5–6
	(500)		1500						1450 °C
[65] 1988	225	0.7 **	1450	20	T,C				3.5
	(500)								1450 °C
[66] 1990 (+500 ppm MgO)	225	0.9–3**	1450	20–30	C	1.3–1.8	ND 620		
	(500)		1500				D 800		
[3] 1990 (+500 ppm MgO)	0	0.8**	1450	20–40	C	1.3	550		
	225	0.65**	1450		C	1.3	600		
	(500)	2.3**	1450				860		
	675	0.8**	1450	Plateau	C	1.6	860		
	(1500)								
[67] 1990	225	1 **	1450	20	C		450		
	(500)			Plateau			750		
681991 (+200 ppm MgO)	800	1	1150	12–39	F, T				
			1250	40–100		1.8	390		
[11] 1993 (+500 ppm MgO)		1 **	1450	20	C	1.3	520	1	5
	0	3 **	1450	20	C	1.1			
	225	1 **	1450	20	C	1.6	600	3	5
	(500)		Plateau	20	C				1450 °C
		3 **	1450	20	C	1.3	800	3	5
[69] 1994	0	3	1125	35–75	T	1.7	453		
			1250		T	1.8			
	1000	2.6	1125	35–75	T	1.7	680		
	(2219)		1250		T				
[4] 1997	0			50	T		483		200
	1000	2.2	1250	50	T		700		1250 °C
	(2219)		1350						
[70] 1998	0	1	1250	50–200	C	2	410		180
	450	1	1250	50–200	C	2	830		1250 °C
	(1000)								
[71] 1999 (+500 ppm MgO)	0	0.8–3.3**	1000	0–15	I. F.		860		
	225	0.7 **	1300	0–15	I. F.		790		
	(500)	2.2 **	1300	0–15	I. F.		970		
	675	0.8 **	1300	0–15	I. F.		1075		
	(1500)			0–15	I. F.				

[a] Grain size values correspond either to the intercept value $\bar{l}$ (*) or to $1.38\sqrt{\bar{s}}$ (**). Other abbreviations are ND, non-doped; D, doped; I. F. Internal Friction.

first assumption on the role of yttrium put forward that yttrium decreases the intergranular diffusion and thus the dislocation climb process kinetics.[66] The same idea of an inhibition of GB diffusion by yttrium was taken up by another group that proposed a site blocking mechanism for rapid transport path.[14] In any case the deformation is not purely Newtonian and GB processes must involve dislocation climb; the decrease in GB diffusion with yttrium segregation was confirmed by diffusion analyses using a radioactive tracer.[72] As for sintering behaviour, yttrium plays a complex role on creep depending on its level and distribution in GBs.

4.3. Influence of the transition between GB segregation and precipitation on creep of alumina

High temperature deformation of fine-grained magnesia and yttria doped alumina presents an "abnormal" "plateau" in the curve giving the creep rate in function of the grain size (Fig. 7). In the usual creep hypothesis of constant microstructure the creep rate must decrease with the grain size. Therefore, the "plateau" regime may be considered as a temporary increase of the deformation rate. This "plateau" appears strongly linked to the evolution of the grain boundary yttrium content. As already mentioned, the grain size increases during deformation and yttrium redistributes itself in a diminishing number of grain boundaries. As a result, yttrium saturation is progressively reached and occurs for an average grain size which just coincides with the grain size at the end of the creep rate "plateau". The presence of a supersaturation just before the precipitation has not been evidenced in these samples but cannot be ruled out. The grain size range of the plateau corresponds roughly to the grain size for which a supersaturation is measured.[25] It is worth noting that the "plateau" is

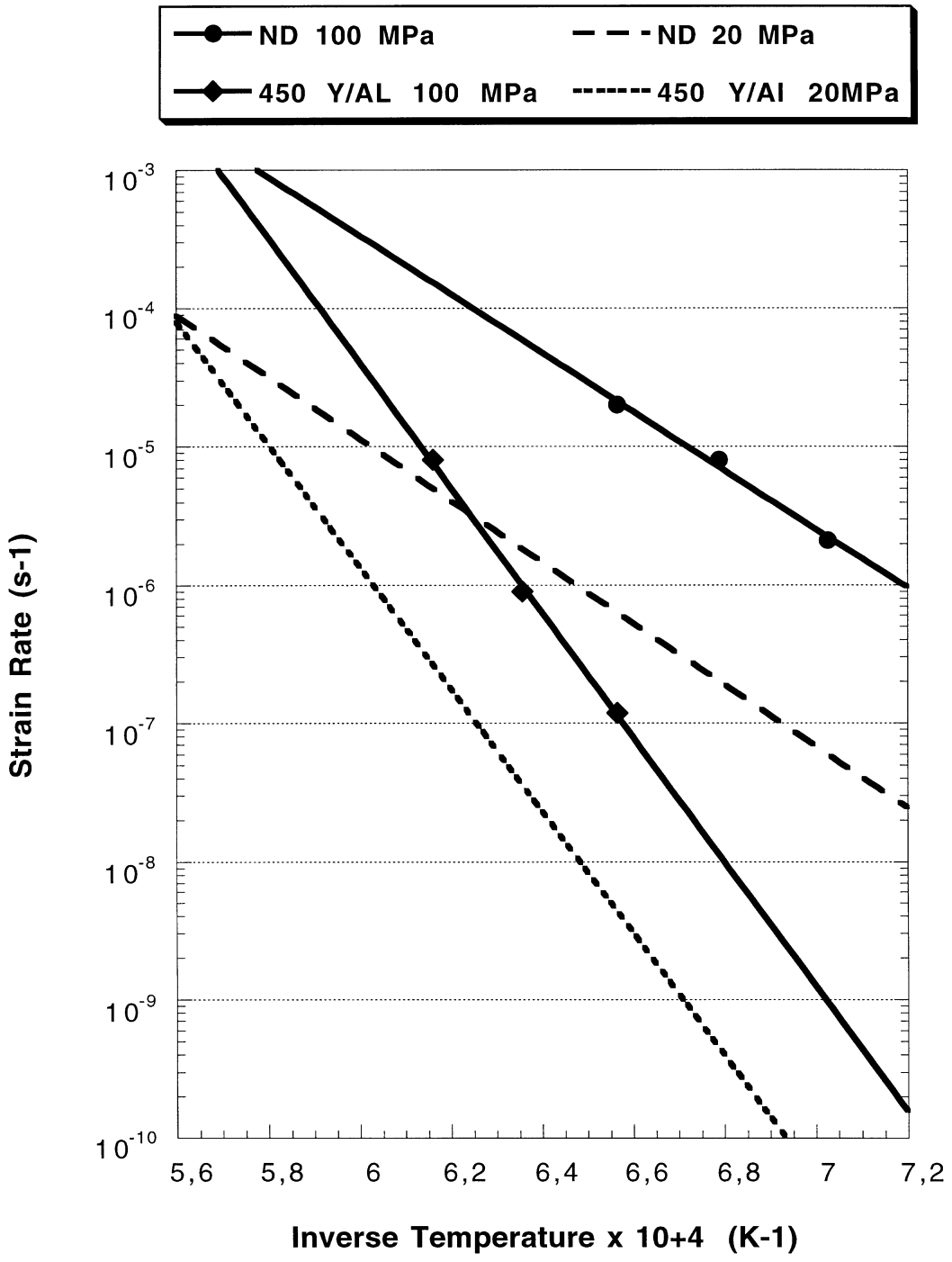

Fig. 6. Creep rates versus inverse of temperature for non doped and 450 ppm Y/Al doped alumina (100 MPa, 1 μm);[70] dashed curves (20 MPa 1 μm) were computed from 100 MPa curves assuming a stress exponent of 2.

shifted towards smaller grain size when the nominal yttrium content increases (Fig. 7). There is obviously a link between the abnormal creep behaviour of alumina and the segregation/precipitation behaviour transition. In order to understand this link, seven deformed samples corresponding to different stages of the curves relating the creep rate versus the grain size were studied by transmission electron microscopy: before the "plateau" (stage A), during the "plateau" stage B), during the strong rate decrease following the "plateau" (stage C), and after the anomaly (stage D; Fig. 8).[11]

The microstructure of the *sintered* samples may be slightly different depending on the grain size. It is equiaxed for grain sizes of 0.65 μm (cf. Fig. 4) and 2.3 μm. For a grain size of 1.9 μm (comprised in the grain size range of the "plateau"), the microstructure contains

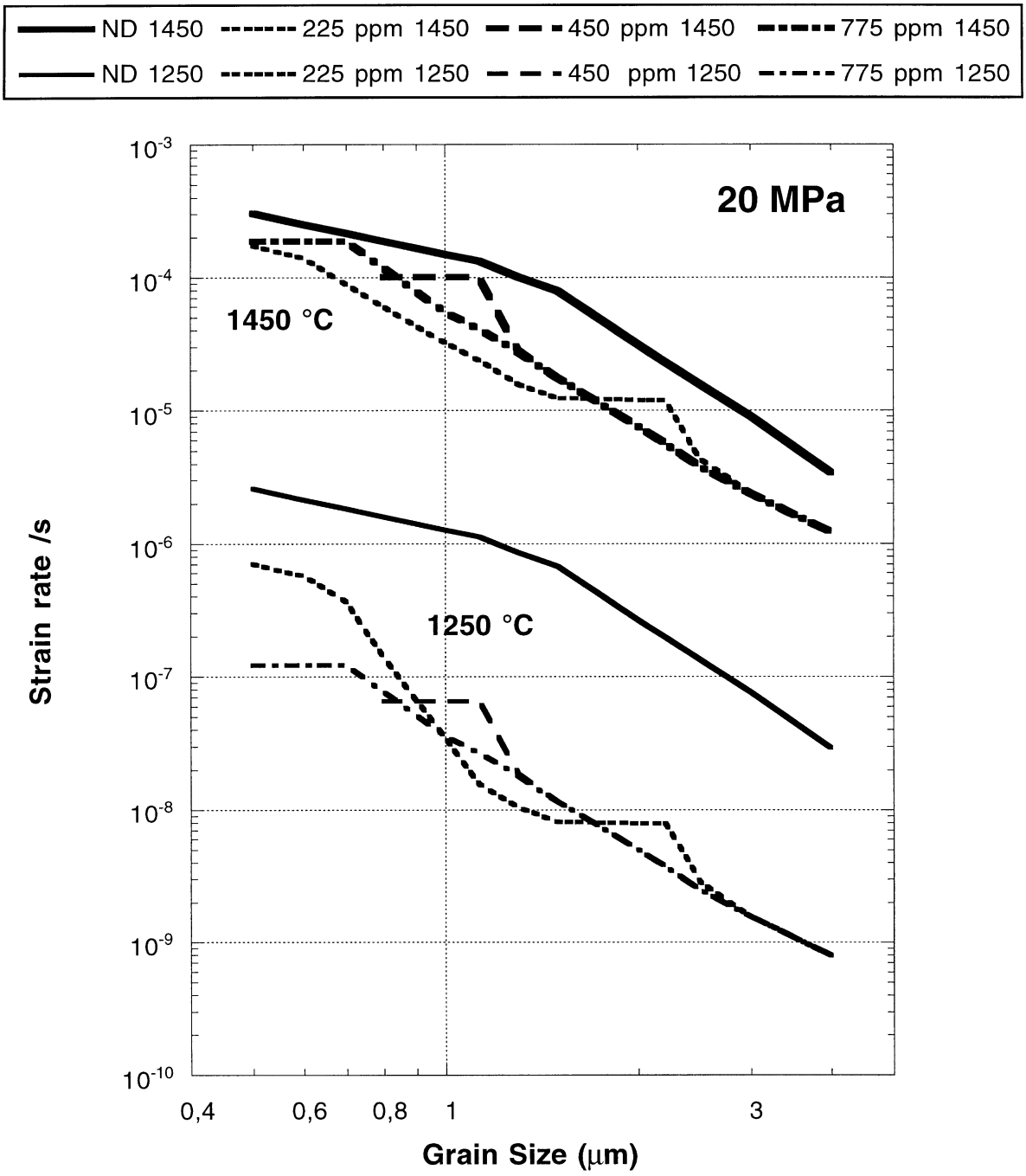

Fig. 7. Creep rates as a function of the grain size for MgO and MgO + Y_2O_3 doped aluminas (20 MPa 1450 °C): dashed curves (20 MPa 1250 °C) were computed from 1450 °C curves using apparent activation energies.[3,53].

slightly elongated grains in some regions of the sample. Simultaneously, the grain boundaries show a tendency to align parallel to the basal plane in one grain. These GBs contain no glassy phase and are faceted at the atomic level; the grain shape heterogeneity is expected to be an unfavourable factor for superplasticity.

The samples *deformed* during the stage A well before the "plateau" and during the stage D well after the "plateau" presents similar microstructures, although grain growth has occurred, except for the presence of YAG precipitates in samples deformed after the "plateau". On the other hand, differences occur in the microstructural features of the samples deformed during the stages B and C that are detailed below. After deformation up to a grain size of 1 μm the microstructures remain equiaxed with a relatively high number of near coincidence GBs. The most striking difference between codoped alumina and alumina doped with only MgO is the presence of numerous dislocations: aperiodic dislocation networks appear both in near coincidence and

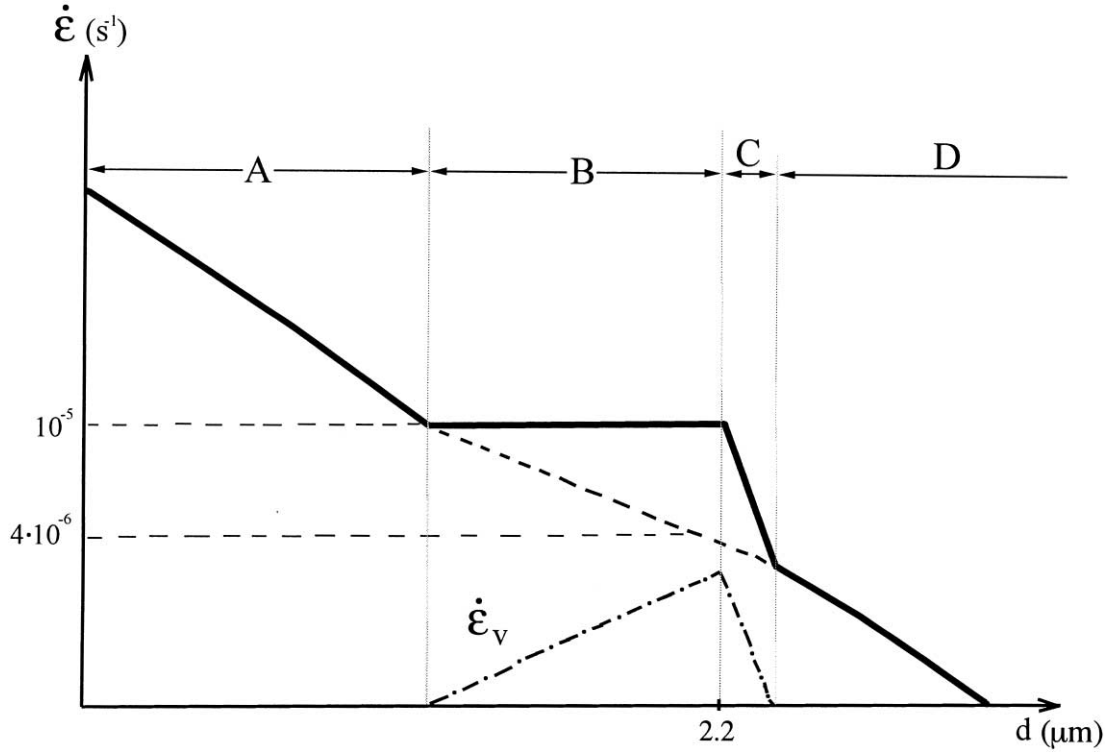

Fig. 8. Creep rates as a function of the grain size for yttrium doped aluminas (225 ppm Y/Al, 500 ppm MgO, 20 MPa 1450 °C). Four stages (A–D) may be defined on the curve. A schematic representation of the contribution of the different mechanisms for the total creep rate is also shown (see Section 5). $\dot{\varepsilon}_v = 6{\cdot}10^{-6}\mathrm{s}^{-1}$ for $d = 2.2$ μm.

"general" GBs (Fig. 9). The microstructures of the samples whose grain sizes correspond to the middle of the "plateau" are similar to those of the sample before the "plateau". A preferential segregation of yttrium on intergranular dislocations has been evidenced in one of these samples,[37] which reveals a strengthening effect of yttrium on the kinetic processes at GBs. It must be noted that a slight elongation of grains occurs after deformation, as in the pressed sample with similar grain size.

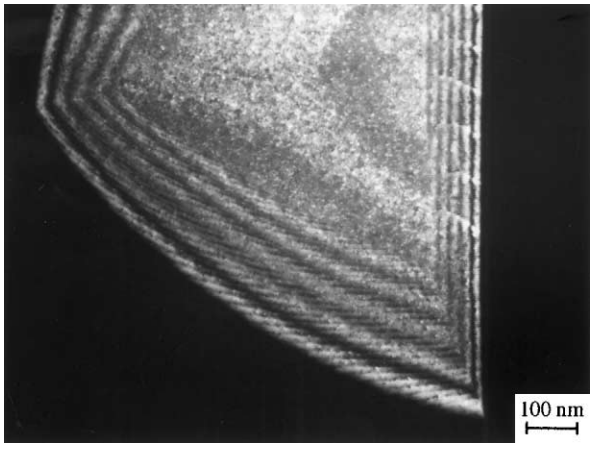

Fig. 9. GB dislocation arrays in $MgO + Y_2O_3$ doped alumina.

The microstructure of the sample deformed just after the "plateau", when the creep rate rapidly decreases, is quite different. It presents a strong dislocation activity in several crystals gathered in some definite regions of the sample. Numerous isolated dislocations occur in GBs and the grains present evidence of basal slip and basal twinning (Fig. 10). The CRSS required to activate basal slip is much larger than the applied stress, implying that GBs are sources for lattice defects. Moreover, some highly deformed grains, often bordered by basal type GB planes, contain dislocations in other slip systems with still higher CRSS. This means that a very high level of internal stresses is attained in some regions of the samples. More surprising is the presence of basal stacking faults bordered by partial dislocations and emitted by GBs (Fig. 11), implying that yttrium must decrease fault energy in the basal plane.[73] In fact this is the first direct observation of the occurrence of grain deformation in superplasticity mechanisms of alumina. This grain deformation is accompanied by a strengthening effect just after the transition segregation/precipitation. This strengthening is confirmed by the microstructures of the samples with a final grain size corresponding to stage D. The sample whose initial grain size corresponds to a stage with only segregation, before the "plateau", still presents dislocation activity, but less pronounced than in the previous sample; basal

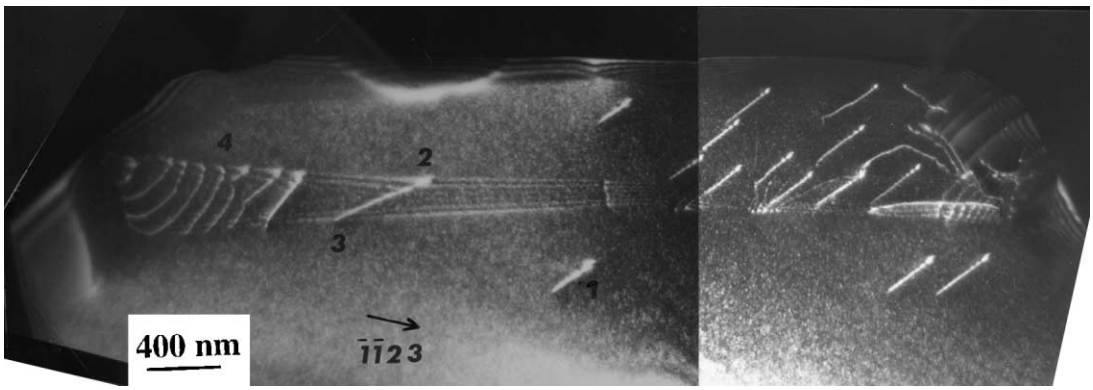

Fig. 10. Dark field image of the microstructure of the $MgO + Y_2O_3$ doped alumina deformed up to the stage C in the deformation curve of the Fig. 8. The grain presents basal slip (dislocations 1) and basal twins. The twin contains twinning dislocations (4 and 2) and basal dislocations (3). The GB at the right end of the micrograph presents numerous extrinsic dislocations.

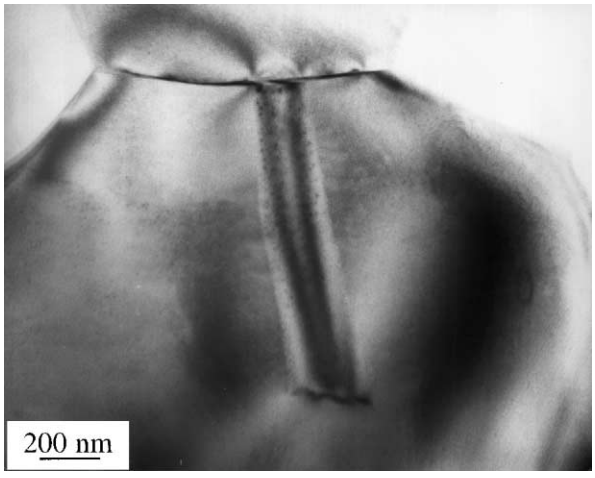

Fig. 11. Basal stacking fault bordered by a partial dislocation in a grain of the $MgO + Y_2O_3$ doped alumina deformed up to the stage C in the deformation curve of the Fig. 8.

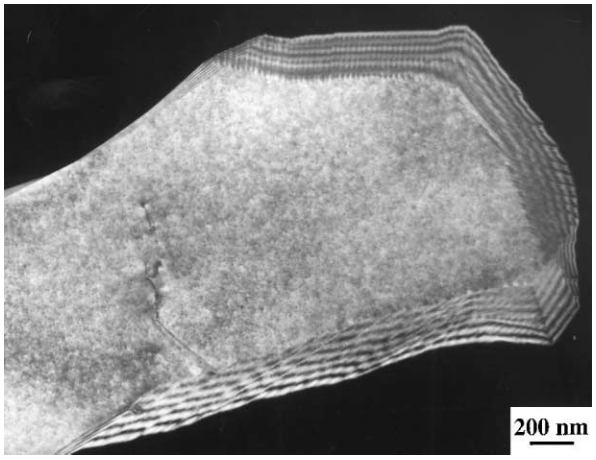

Fig. 12. Dislocation networks in the GBs of a sample deformed up to the stage D, well after the "plateau" regime.

slip and basal microtwins occur in grains most often slightly elongated. On the contrary, the microstructure of the sample whose initial grain size corresponds to the end of the "plateau" is similar to those of the samples deformed before the "plateau". The strong lattice dislocation activity is suppressed and GB dislocations are arranged as arrays (Fig. 12). The grains are equiaxed. Similar observations have been made on the sample with still larger grain size; thus the transition from a GB segregation to a GB precipitation induces striking modifications in the creep behaviour that are tentatively interpreted in the next section.

5. Discusssion

The mechanisms that occur during the different stages of deformation of the fine-grained aluminas doped with yttria are described on the basis of the superplasticity models. The contribution of each mechanism to the total creep is schematically reported in Fig. 8. During stage A, GB sliding is accommodated by GB diffusion in agreement with a grain size exponent p equal to 3 (cf. Section 4.2). GB diffusion is coupled with climb motion of GB dislocations. Yttrium decreases intergranular dislocation climb kinetics by decrease in the GB diffusivity. Dislocation mobility is reduced in GBs and there is no lattice dislocation activity inside the grains. Thus the main contribution to the GB sliding rate is the GB diffusion rate $\dot{\varepsilon}_s = \dot{\varepsilon}_b + \dot{\varepsilon}_{cr}$. As $\dot{\varepsilon}_b$ is proportional to σ^2 and $\dot{\varepsilon}_{cr}$ is proportional to σ, the mean n value may have an intermediate value between 1 and 2.

During stage B, the Y content in the GBs increases. GB dislocations are stabilised by yttrium segregation as it has been revealed by STEM analyses.[37] The accommodation processes within GBs are now difficult. Relaxation occurs by emission of lattice dislocations that can be absorbed by opposite GBs. These dislocations are not observed because they rapidly cross the small grains. But the activation of basal slip is supported by the grain

elongation and by the basal texture observed at the mesoscopic scale.[23] According to the "fluid like model", the increase in the flux of lattice dislocations leads to an overlapping of fluid like regions and the formation of a highly excited state for the GBs. The shear potential relief decreases and the GB diffusivity increases such as $D_b = D_{b0}(1 + k\dot{\varepsilon})$.[61] The strain rate takes now a new component $\dot{\varepsilon}_v$ in the total strain rate $\dot{\varepsilon} = \dot{\varepsilon}_b + \dot{\varepsilon}_v + \dot{\varepsilon}_{cr}$. Estimation of the lattice dislocation activity at the end of the plateau regime has been made using Taylor's law: $\dot{\varepsilon}_v = \alpha \cdot \rho_m \cdot b \cdot \bar{v}$ in which $\alpha = 0.25$, ρ_m is the density of mobile dislocations in the crystals, b the amplitude of their Burgers vector and $\bar{v}$ their average glide rate. $\dot{\varepsilon}_v$ has been estimated as the difference between the experimental curve (the total creep rate) and the extrapolated rate curve due to diffusion (Fig. 8). By assuming a plausible value of the dislocation motion velocity $\bar{v} = 10^{-6}\text{ms}^{-1}$ or 10^{-7}ms^{-1},[74] the calculated density of mobile dislocations takes a reasonable value: $\rho_m = 10^{11} - 10^{12}\text{m}^{-2}$.

In stage C, just after the plateau, GBs are saturated with yttrium. Extrinsic dislocations are stabilised by segregation and the GBs can no longer absorb lattice dislocations. As a result the stresses remain concentrated within some grains. The high dislocation activity revealed by TEM could explain the hardening effect observed on the creep rate curve. $\dot{\varepsilon}_v$ decreases rapidly and the total creep rate is strongly reduced.

In stage D, the lattice dislocation activity disappears and simultaneously the slope of the creep rate curve becomes identical to that of part A. The presence of sub grain boundaries within several crystals suggests the occurrence of a dynamic recovery process. Indeed, competition between deformation and relaxation at high temperature is plausible at the low strain rates reached in that stage.

An alternative explanation may also account for the enhancement of creep rate during the "plateau". As already mentioned, yttrium modifies sintering behaviour but also anelastic and viscoplastic deformation. Internal friction measurements on the same alumina codoped with Y and Mg reveal the same trends as those obtained by creep.[71] In that case the most likely mechanism of deformation is the motion of GB dislocations; as a matter of fact no intragranular dislocation activity could occur at the low stresses and temperatures of the tests, nor a long-range diffusional accommodation. Of particular interest is the enhanced mechanical loss concurrent with the saturation of GBs with yttrium.[71] It was interpreted by an enhanced GB diffusivity, and a continuously changing GB microstructure during saturation and before precipitation. The strong modification of the microstructures around the transition between yttrium GB segregation and precipitation of yttrium aluminium garnet,[25] and the increase in sintering rate for this same transition[5] support a transient change in diffusional behaviour. The hypothesis of a disordered GB region with yttrium supersaturation before the transition is in agreement with a transient increase in diffusion. Nevertheless, this hypothesis must be considered with caution in so far as the results on GB segregation in metals merely suggest the formation of an ordered two dimensional compound in the interface.[75] A transient increase in the boundary width δ, deduced from EXAFS experiments,[27] also increases the product δD and may play a role in the kinetics of creep and sintering. An increase of this product has a similar effect as an increase in the diffusion coefficient. The microstructural features of highly doped aluminas with bimodal microstructure can be understood from this assumption. GBs are not saturated with yttrium at the same moment during grain growth. First saturated GBs may display higher migration rates than other non saturated GBs. Rapid diffusion of yttrium (yttrium GB diffusion is five order of magnitude greater than self diffusion in alumina[76]) occurs towards nucleation sites mostly located at some triple points bounding the areas where a local preferential grain growth occurs. The precipitates then impede growth of smaller grains remaining in the microstructure by a pinning effect. An anisotropy of grain shape occurs in the presence of silicon with predominance of the basal type GB plane (Section 2). Such an anisotropy is not observed when Mg is added; this element plays a homogenising role toward GB segregation and limits grain growth.[77] Nevertheless, grain elongation occurs during the plateau despite the presence of magnesium. At the saturation stage, strong variations in GB chemistry from one GB to another must occur with probably site competition effects.

6. Concluding remarks

The main effect of yttrium doping on alumina polycrystal microstructures and behaviours at high temperatures are summed up as follows: yttrium decreases the alumina densification and creep rates. The transition between yttrium GB segregation and precipitation of garnets within the GBs is associated with anomalies of densification and creep rates. These two effects are strongly linked to the microstructure with a particular emphasis on the change in the GB microchemistry and structure. As soon as precipitation occurs in GBs, the decrease in creep rate no longer depends on the dopant concentration. This decrease is more striking at lower temperature, owing to the large apparent activation energy.

At much lower temperature (ambient), when the diffusional mechanisms cannot operate, the differences between the mechanical properties of doped and non-doped alumina still exist. In particular, the toughness of

polycrystals displaying GB saturated with yttrium is significantly higher than those of non-doped alumina.

For other doping elements with low solubility in alumina (La, Ti, Zr. . .etc.), similar microstructural transition between GB segregation and GB precipitation should exist; anomaly on sintering rates has effectively been observed for titanium doped alumina.[78] Such transition with increasing grain size has been reported in another oxide (TiO_2) doped with calcium.[79] It probably could occur in most oxide polycrystals with rather anion closed packed structure and low doping element solubility.

Codoping effects on such microstructural transition and thus on macroscopic behaviours should be studied on powders and materials with a level of residual impurity carefully controlled.

Finally these results open the way to further design of nanograined alumina. In that case, the highest doping level inducing only GB segregation should increase with decreasing grain sizes. However this limit level has to be investigated on samples prepared with powders doped at the precursor level and carefully processed. The effect of very high GB densities in nanograined material properties has to be explored carefully as any extrapolation from micrograined material behaviour is hazardous.

For an intermediate temperature practical application such as the translucent alumina tube of sodium lamps it should be interesting to use materials with only GB segregated microstructure: the 1968 US patent[46] claim is a very good illustration of such an adequate doping level (Y and Mg) and grain size combination.

References

1. Heuer, A. H., Tighe, N. J. and Cannon, R. M., Plastic deformation of fine grained alumina, II, Basal slip and nonaccomodated grain-boundary sliding. *J. Am. Ceram. Soc.*, 1980, **63**, 53–58.
2. Le Gall, M., Huntz, A. M., Lesage, B., Monty, C. and Bernardini, J., Self-diffusion in α-Al_2O_3 and growth rate of alumina scales formed by oxidation: effect of Y_2O_2 doping. *J. Mater. Sci.*, 1995, **30**, 201–211.
3. Gruffell, P. and Carry, C., Strain rate plateau in creep of yttria doped fine grained alumina. In *Structural Ceramics—Processing, Microstructure and Properties*, ed. J. J. Bentzen *et al.* Risø National Laboratory, Roskilde, DK, 1990, pp. 305–311.
4. Cho, J., Harmer, M. P., Chan, H., Rickman, J. M. and Thompson, A. M., Effect of yttrium and lanthanum on the tensile creep behavior of aluminium oxide. *J. Am. Ceram. Soc.*, 1997, **80**, 1013–1017.
5. Sato, E. and Carry, C., Yttria doping and sintering of sub-micron grained α-alumina. *J. Am. Ceram. Soc.*, 1996, **79**, 2156–2160.
6. Lartigue, S. and Priester, L., Analysis of grain boundaries in fine-grained Mg-doped aluminas. In Grain Boundary Structure and Related Phenomena. *Transaction of JIMIS*, 1986, **27**, 205–212.
7. Lartigue, S. and Priester, L., Grain boundaries in fine grained Mg doped aluminas with different microstructures. *J. Am. Ceram. Soc.*, 1988, **71**, 430–437.
8. Priester, L. and Lartigue, S., Description and role in high temperature deformation of grain boundaries in an alumina ceramic. *J. Eur. Ceram. Soc.*, 1991, **8**, 47–57.
9. Gülgün, M. A., Putlayev, V. and Rühle, M., Effect of yttrium doping α-alumina: I. Microstructure and microchemistry. *J. Am. Ceram. Soc.*, 1999, **82**, 1849–1856.
10. Bruley, J., Cho, J., Chan, H. M., Harmer, M. P. and Rickman, J. M., Scanning electron microscopy analysis of grain boundaries in creep-resitant yttrium and lanthanum-doped alumina microstructures. *J. Am. Ceram. Soc.*, 1999, **82**, 2865–2870.
11. Lartigue, S., Priester, L., Dupau, F., Gruffel, P. and Carry, C., Dislocation activity and differences between tensile and compressive creep of yttria doped alumina. *J. Mater. Sci. Eng.*, 1993, **A164**, 211–215.
12. Lartigue Korinek, S. and Dupau, F., Grain boundary behavior in superplastic Mg-doped alumina with yttria codoping. *Acta Metall. Mater.*, 1994, **42**, 293–302.
13. Priester, L., Dupau, F., Lartigue Korinek, S. and Carry, C., On the relationships between the constitutive creep laws and the microstructural behavior of alumina polycrystals. Interface science and materials interconnection. Proceedings of JIMIS. *The Japan Institute of Metals*, 1996, **8**, 134–142.
14. Cho, J., Wang, C. M., Chan, H. M., Rickman, J. M. and Harmer, M. P., Role of segregating dopants on the improved creep resistance of aluminium oxide. *Acta Mater.*, 1999, **47**, 4197–4207.
15. Lartigue, S. and Priester, L., Stability of extrinsic grain boundary dislocations in relation with intergranular segregation and precipitation. *Acta Metall.*, 1983, **31**, 1809–1819.
16. Nanni, P., Stoddart, C. T. H. and Hondros, E. D., Grain boundary segregation and sintering in alumina. *Materials Chemistry*, 1976, **1**, 297–320.
17. Johnson, W. C., Grain boundary segregation in ceramics. *Met. Trans.*, 1977, **8A**, 1413–1421.
18. Bender, B., Williams, D. and Notis, M., Investigation of grain-boundary segregation in ceramic oxides by analytical scanning transmission electron microscopy. *J. Am. Ceram. Soc.*, 1980, **63**, 542–546.
19. Li, C. W. and Kingery, W. D., Solute segregation at grain boundaries in polycrystalline Al_2O_3, Advance in Ceramics, ed. W. D. Kingery. *Am. Ceram. Soc. Ohio*, 1984, **10**, 368–378.
20. Cawley, J. D. and Halloran, J. W., Dopant distribution in nominally yttrium-doped sapphire. *J. Am. Ceram. Soc.*, 1986, **69**, C195–C196.
21. McCune, R. C., Donlon, W. T. and Ku, R. C., Yttrium segregation and YAG precipitation at surfaces of yttrium-doped α-Al_2O_3. *J. Am. Ceram. Soc.*, 1986, **69**, C196–C199.
22. Ching, W. Y., Xu, Y. N. and Rühle, M., Ab-initio calculation of yttrium substitutional impurities in α-Al_2O_3. *J. Am. Ceram. Soc.*, 1997, **80**, 3199–3204.
23. Gruffel, P. and Carry, C., Effect of grain size on yttrium grain boundary segregation in fine grained alumina. *J. Euro. Ceram. Soc.*, 1993, **11**, 189–199.
24. Carry, C., Bowen, P., Herbst, F. and Legros, C., The effect of yttrium and zirconium on sintering of a transition alumina. In *Sintering Science and Technology*, ed. R. M. German, G. L. Messing and R. G. Cornwall. The Pennsylvania State University, State College, PA, USA, 2000, pp. 177–182.
25. Gülgün, M. A. and Rühle, M., Yttrium in polycrystalline α-alumina. *Key Engineering Materials*, 2000, **171–174**, 793–800.
26. Wang, C. M., Cargill, G. S., Harmer, M. P., Chan, H. M. and Cho, J., Atomic structural environment of grain boundary segregated Y and Zr creep resistant alumina from EXAFS. *Acta Mater.*, 1999, **47**, 3411–3422.
27. Wang, C. M., Cargill, G. S. III, Chan, H. M. and Harmer, M. P., Structural features of Y-saturated and supersaturated grain boudaries in alumina. *Acta Mater.*, 2000, **48**, 2579–2591.
28. Takigawa, Y., Ikuhara, Y. and Sakuma, T., Grain boundary bonding state and fracture energy in small amount of oxide-doped fine-grained Al_2O_3. *J. Mater. Sci.*, 1999, **34**, 1991–1997.
29. Gülgün, M. A., Ching, W. Y. and Rühle, M., Yttrium-segregated

grain boundaries in α-Al_2O_3: an EELS study. *Materials Science Forum*, 1999, **294–296**, 289–292.
30. Loudjani, M. K. and Cortes, R., X-ray adsorption spectrocopy study of the local structure and the chemical state of yttrium in polycrystalline alpha alumina. *J. Eur. Ceram. Soc.*, 1994, **14**, 67–75.
31. Kenway, P. R., Calculated structures and energies of grain boundaries in alpha Al_2O_3. *J. Am. Ceram. Soc.*, 1994, **77**, 349–355.
32. Mo, S. D. and Ching, W. Y., Electronic structure of a near sigma 11 a-axix tilt grain boundary in alpha Al_2O_3. *J. Am. Ceram. Soc.*, 1996, **79**, 627–633.
33. Exner, M. and Finnis, M. W., Atomic simulation of grain boundaries in alumina. *Mat. Science Forum, Transtec Pub. Switzerland*, 1996, **207-209**, 225–228.
34. Cho, J., Rickman, J. M., Chan, H. M. and Harmer, M. P., Modeling of grain-boundary segregation behavior in aluminium oxide. *J. Am. Ceram. Soc.*, 2000, **83**, 344–352.
35. Yoshida, H., Ikuhara, Y. and Sakuma, T., High-temperature creep resistance in lanthanoid ion-doped polycrystalline Al_2O_3. *Philos. Mag. Letters*, 1999, **79**, 249–256.
36. Sutton, A. P. and Balluffi, R. W., *Interfaces in Crystalline Materials*. Clarendon Press, Oxford, 1995.
37. Bouchet, D., Dupau, F. and Lartigue-Korinek, S., Structure and chemistry of grain boundaries in yttria doped aluminas. *Microsc. Microanal. Microstruct.*, 1993, **4**, 561–573.
38. Mackrodt, W. C., The calculated equilibrium segregation of Fe^{3+}, Y^{3+}, and La^{3+} at the low-index surfaces of α-Al_2O_3. In *Advances in Ceramics. Nonstoichiometric Compounds,* Vol. 23, ed. C. R. A. Catlow and W. C. Mackrodt. Am Ceram Soc, Westville, OH, 1987, pp. 239–306.
39. Loudjani, M. K. and Haut, C., Influence of the oxygen pressure on the chemical state of yttrium in polycrystalline α-alumina. Relation with microstructure and mechanical properties. *J. Europ. Ceram. Soc.*, 1996, **16**, 1099–1106.
40. Lartigue, S. and Priester, L., Influence of doping elements on the grain boundary characteristics in alumina. *J. de Physique*, 1988, **C5-49**, 451–456.
41. Lartigue, S., *Influence des dopants et de la déformation à chaud sur les paramètres cristallographiques des joints de grains et les dislocations intergranulaires dans l'alumine*. Doctorat d'Etat thesis, Orsay, France, 1988.
42. Cho, J., Chan, H. M., Harmer, M. H. and Rickman, J. M., Influence of yttrium doping on grain misorientation in aluminium oxide. *J. Am. Ceram. Soc.*, 1998, **81**, 3001–3004.
43. Brandon, D. G., The structure of high angle grain boundaries. *Acta Metall.*, 1966, **14**, 1479.
44. Grimmer, H., Bonnet, R., Lartigue, S. and Priester, L., Theoretical and experimental descriptions of grain boundaries in rhombohedral alumina. *Philos. Mag.*, 1990, **A61**, 493–509.
45. Coble, R. L., *Transparent Alumina and Method of Preparation*. US Patent No. 3,026,210, 1962.
46. Wolkodoff, V. E. and Weaver, R. E., *Alumina Ceramic*, US Patent No. 3,377,176, April 9 1968.
47. Kobayashi, K. and Kaneno, M., *Utilzing Mixtures of Yttria, Magnesia, and Lanthanium Oxide in Manufacture of Transparent Alumina*. US Patent No. 3,792,142, February 12 1974.
48. Kobayashi, K. and Kameno, M., *Translucent Alumina Containing Magnesia Yttria and Lanthium Oxide*, US Patent No. 3,905,845, September 16 1975.
49. Delaunay, D., Huntz, A. M. and Lacombe, P., The influence of yttrium on the sintering of alumina. *J. Less-Common Metals*, 1980, **70**, 115–117.
50. Fang, J., Thompson, A. M., Harmer, M. P. and Chan, H. M., Sintering behavior of ultra-high purity Al_2O_3 doped with Y and La. In *Sintering Technology*, ed. R. M. German, G. L. Messing and R. G. Cornwall. M. Dekker, 1996, pp. 317–324.
51. Fang, J., Thompson, A. M., Harmer, M. P. and Chan, H. M., Effect of yttrium and lanthanum on the final-stage sintering of ultrahigh-purity alumina. *J. Am. Ceram. Soc.*, 1997, **80**, 2005–2012.
52. Sato, E. and Carry, C., Effect of yttrium doping on sintering of fine grained alumina. In *Third Euro-Ceramics, Vol. 1*, ed. P. Duran and J. F. Fernandez. Faenza, Iberica S.L., Spain, 1993, pp. 691–696.
53. Sato, E. and Carry, C., Sintering and yttrium grain boundary segregation in sub micron grain size alumina. In *Euromat*, Vol. 3, Chapter 7, ed. R. Pichoir and P. Costa. Journal de Physique, pp. 1335–1340.
54. Carry, C. and Mocellin, A., High ductilities in fine grained ceramics. In *Superplasticity*, Editions du C.N.R.S., 1985, pp. 16.1–16.19.
55. Hah, S. R., Fischer, T. E., Gruffel, P. and Carry, C., Effect of grain boundary dopants and mean grain size on tribomechanical behavior of highly purified α-alumina in the mild wear regime. *Wear*, 1995, **181-177**, 165–177.
56. Cannon, R. M., Rhodes, W. H. and Heuer, A. H., Plastic deformation of fine grained alumina: I, Interface-controlled diffusion creep. *J. of Am. Ceram. Soc.*, 1980, **63**, 46–53.
57. Pond, R. C., Smith, D. A. and Southerdern, P. W. J., On the role of grain boundary dislocations in high temperature creep. *Philos. Mag.*, 1978, **A37**, 27.
58. Valiev, R. Z., Gertsman, V. Y. and Kaibystshev, O. A., Non-equilibrium state and recovery of grain boundary structure. *Phys. Stat. Sol.*, 1983, **A77**, 97–111.
59. Priester, L., On the accommodation of extrinsic dislocations in grain boundaries. *Interface Science*, 1997, **4**, 205–219.
60. Vetrano, J. S., Simonen, E. P. and Bruemmer, S. M., Evidence for excess vacancies at sliding grain boundaries during superplastic deformation. *Acta Mater.*, 1999, **47**, 4125–4129.
61. Perevezentsev, V. N., Rybin, V. V. and Chuvil'deev, V. N., Overview No. 97. The theory of structural superplasticity. *Acta Metall.*, 1992, **40**, 887–914.
62. Thompson, A. M., Soni, K. K., Chan, H. M., Harmer, M. P., Williams, D. B., Chabala, J. M. and Levi-Setti, R., Dopant distribution in rare-earth-doped alumina. *J. Am. Ceram. Soc.*, 1997, **80**, 373–376.
63. Carry, C. and Mocellin, A., Superplastic forming of alumina. *Proceedings of the British Ceramic Society*, 1983, **33**, 101–115.
64. Carry, C. and Mocellin, A., Structural superplasticities in single phase crystalline ceramics. *Ceramics International*, 1987, **13**, 89–98.
65. Gruffel, P., Carry, C. and Mocellin, A., Effect of testing conditions on superplastic creep of alumina doped with Ti and Y. *Science of Ceramics, The Institute of Ceramics, UK*, 1988, **14**, 587–592.
66. Lartigue, S., Carry, C. and Priester, L., Grain boundaries in high temperature deformation of yttria and magnesia co-doped alumina. *Journal de Physique, Colloque C1*, 1990, **51**, C1985–C1990.
67. Streit, P., *Plasticité à haute température d'alumines à grains fins dopées à l'Yttrium ou au Lanthane*, Projet de Diplôme, Ecole Polytechnique Fédérale de Lausanne, Suisse, 1990.
68. Robertson, A. G., Wilkinson, D. S. and Caceres, C. H., Creep and creep fracture in hot-pressed alumina. *J. Am. Ceram. Soc.*, 1991, **74**, 915–921.
69. French, J. D., Zhao, J., Harmer, M. P., Chan, H. M. and Miller, G. A., Creep of duplex microstructures. *J. Am. Ceram. Soc.*, 1994, **77**, 2857–2865.
70. Yoshida, H., Ikuhara, Y. and Sakuma, T., High-temperature creep resistance in lanthanoid ion-doped polycrystalline Al_2O_3. *Journal of Materials Research*, 1998, **13**, 2597–2601.
71. Lakki, A., Schaller, R., Carry, C. and Benoit, W., High temperature anelastic and viscoplastic deformation of fine-grained

magnesia and magnesia/yttria-doped alumina. *J. Am. Ceram. Soc.*, 1999, **82**, 2181–2187.
72. Prot, D., Le Gall, M., Lesage, B., Huntz, A. M. and Monty, C., Self-diffusion in undoped and yttria-doped alumina polycrystals. *Philos. Mag.*, 1996, **A73**, 935–949.
73. Heuer, H. and Castaing, J., Dislocations in α-Al_2O_3. In *Advances in Ceramics*, ed. W. D. Kingery. Am Cer Soc, Columbus, Ohio, 1985, pp. 238–257.
74. Komatsu, M., Mori, H. and Iwasaki, K., Titre à trouver. *J. Am. Ceram. Soc.*, 1994, **77**, 839–842.
75. Guttmann, M. and McLean, D., "*Interfacial Segregation*", ed W. C. Johnson and J. M. Blakely, 1979, p. 261.
76. Moya, E. G., Moya, F., Lesage, B., Loudjani, M. K. and Grattepain, C., Yttrium diffusion in alpha-alumina single crystal. *J. Eur. Ceram. Soc.*, 1998, **18**, 591–594.
77. Gavrilov, K. L., Bennison, S. J., Mikeska, K. R., Chabala, J. M. and Levi-Setti, R., Silica and magnesia dopant distributions in alumina by high resolution scanning secondary ion mass spectrometry. *J. Am. Ceram. Soc.*, 1999, **82**, 1001–1008.
78. Herbst, F., Legros, C., Lartigue-Korineck, S. and Carry, C., *Grain Boundary Segregation and Precipitation Map for Doped Alumina*. To be published and presented at the European Ceramic Society Conference, Brugges, Belgium, September 2001.
79. Terwilliger, C. D. and Chiang, Y.-M., Size-dependent solute segregation and total solubility in ultrafine polycrystals: Ca in TiO_2. *Acta Metall. Mater.*, 1995, **43**, 319–328.